

Two-electron excitations and one-electron multiple-scattering resonances in the x-ray absorption of solid neon

A. V. Soldatov*

Dipartimento di Fisica, Università di Roma, "La Sapienza," 00185 Roma, Italy

T. S. Ivanchenko

Department of Solid State Physics, Rostov University, Sorge strasse 5, 344104 Rostov-Don, Russia

S. Della Longa and A. Bianconi

Universita dell'Aquila, via S. Sisto 20, 67100 L'Aquila, Italy

and Dipartimento di Fisica, Università di Roma, "La Sapienza," 00185 Roma, Italy

(Received 6 July 1992; revised manuscript received 27 October 1992)

The local and partial density of states of the conduction band of solid neon in a large energy interval has been extracted from the analysis of the K -edge x-ray-absorption near-edge structure (XANES) spectrum by using a full multiple-scattering method. The absorption cross section for one-electron transitions from the Ne $1s$ level to the conduction-band final states in the solid Ne is predicted by first principles. The absorption cross section is described as due to an atomic factor and to a structure factor determined by the local and partial density of states for a large cluster formed by about 80 atoms. The experimental spectrum is obtained by describing the final state in the fully relaxed potential in the presence of the core hole. The exciton peak at threshold is shown to be due to the lowest unoccupied valence state pushed down in the bound-state region by the core hole. In the 100-eV XANES energy range the single-scattering approximation fails to predict the XANES of solid Ne indicating that the full multiple-scattering approach is required. The present analysis allows us to identify strong two-electron excitations $1s^2 2s^2 2p^6 \rightarrow 1s^1 2s^2 2p^5 \epsilon_i p^2$ in the energy range of 30 eV above the K edge, involving monopole $2p \rightarrow \epsilon p$ transitions to the lowest valence states at energy ϵ . The intensity of the two-electron excitations is found to be so strong that it should be considered in standard extended x-ray-absorption fine-structure-XANES data analysis for local structure investigation.

I. INTRODUCTION

The core-level photoionization in the x-ray-absorption spectra (XAS) giving the x-ray-absorption near-edge structure (XANES) and the extended x-ray-absorption fine structure (EXAFS) are intrinsic many-body excitations. The one-electron approximation, where the electron in the core level that is excited into the unoccupied states is separated from the $N - 1$ passive electron, is able to give account of the major features in the experimental spectra.^{1,2} One of the most important multielectron processes that contributes to the x-ray-absorption spectra is the two-electron excitation. This phenomenon is well known in the core photoabsorption spectra of atoms. The double-electron excitations have been found in atomic K -edge absorption spectra of rare gases Ar,³⁻⁶ Ne,^{7,8} Kr,⁹ Xe,¹⁰ sodium vapor,¹¹ and in gas-phase SiX_4 ($X = \text{H}, \text{CH}_3, \text{F}, \text{Cl}, \text{Br}$) molecules.¹² The many-body effects in the atomic spectra can be described by the theory of configuration interaction between different photoabsorption channels contributing to the total cross section.¹³ Discrete multielectron features in the x-ray atomic spectra are due to the trapping of two electrons in Ry states, and they can be easily identified because they appear in the continuum smooth atomic absorption for the elastic one-electron channel above the ionization potential of the core hole.

In the solid-state spectra, only weak features¹⁴ have been found to correspond to double-electron excitations in α -SiH,¹⁵ Ni,¹⁶ Ge,¹⁷ Ne,¹⁸ Pr and Sm,¹⁹ Cu,²⁰ RbBr and β -PbO₂,²¹ and V, Cr, and Mn tetrahedral complexes.²² Because the elastic one-electron channel generally dominates in the XANES region, one needs to identify first the strong one-electron spectral features in order to find the weak contributions due to two-electron excitations.

In condensed rare-gas solids, where the van der Waals interactions between atoms are dominant,²³ it is of particular interest to compare the two-electron excitations in the gaseous spectrum with that in the solid-state spectrum.²⁴

The x-ray-absorption spectra of solid rare gases were measured mostly in the soft-x-ray region of electronic transitions from shallow core levels $2p$ ($L_{2,3}$), $3p$ ($M_{2,3}$), or $3d$ ($M_{4,5}$) (Refs. 25-27) to unoccupied localized d and f states, where one must take into account strong correlation effects,²⁸ and the spectra have a dominant atomic-like character. Recently the x-ray-absorption near-edge structure (XANES) in the K -edge spectrum of solid Ne has been measured²⁹ at low temperature (6.3 K), with good energy resolution. The XANES spectrum exhibits well-resolved spectral features, due to the narrow Ne $1s$ core-level width. The K -edge XANES spectra of other heavy rare gases have been measured (see, for example,

Ref. 30), but because of the large core-hole energy width or poor energy resolution these spectra exhibit very broad features.

In this work, we have addressed our interest to solid neon K -edge XANES data,²⁹ as a good spectrum to test the following.

(i) The *ab initio* one-electron full multiple-scattering approach to calculate the XANES spectrum, including the continuum- and bound-state energy range, by using a recent computer code G4XANES developed by our group.

(ii) The application of our approach to obtain the spectrum of the partial density of states with selected orbital angular momentum.

(iii) The investigation of the variations of the two-electron excitations from the gas phase to the solid phase.

(iv) The estimation of the intensity of double-electron excitations in the EXAFS (XANES) region that have to be identified and eliminated in the structural determination by using standard EXAFS (XANES) analysis.

II. THE G4XANES COMPUTATIONAL APPROACH

It has been well established that the calculation of x-ray-absorption spectra by full multiple scattering in real space³¹ is equivalent to the exact calculations of the absorption cross section for core transitions, given in the one-electron approximation by the product of the matrix element and the joint density of states, in accord with the Fermi golden rule in k space. In the full multiple-scattering approach in real space, the absorption coefficient can be expanded into an infinite series;

$$\alpha = \alpha_0 \left[1 + \sum_{n=2} \mathcal{X}_n \right],$$

where each term \mathcal{X}_n is the modulation factor due to the photoelectron scattering pathways, including the $n - 1$ neighbor atoms and the central atom.^{1,2}

In the XANES energy region, about 50–100 eV depending on the system, the full multiple-scattering approach is required, while in the high-energy EXAFS region it is possible to neglect the high-order terms in approximating the absorption cross section, considering only the first term \mathcal{X}_2 , due to the pair correlation function, and the second term due to the triplet correlation function \mathcal{X}_3 (see Ref. 22). Going to lower energies, the amplitude of the higher-order terms $\mathcal{X}_{n>3}$ increases gradually, and their relative contribution increases in a complex way due to the cluster geometry, distances, and interference effects. In the low-energy range (50–100 eV) above the absorption threshold, it is not possible to establish “*a priori*” the highest multiple-scattering term to be included in the approximation. On the other hand, the interpretation of the experimental spectra in term of individual \mathcal{X}_n terms becomes very complex where higher-order terms $n \geq 4$ are included. Therefore we think that the best approach to interpreting the XANES data is to calculate the correct spectrum by the full multiple-scattering approach.

It is well known that the final spectrum calculated by the multiple-scattering approach depends on many pa-

rameters required by the calculation (1,2,21,31). We have recently developed a computer package G4XANES, where we have reduced to a minimum the arbitrary choices in the construction of the potential. We use the XANES code developed by Durham and Pendry²¹ to calculate the multiple-scattering spectrum. The inputs of the program are (1) the crystal symmetry, (2) the lattice parameters, (3) the central atom, and (4) the cluster size. First, the program calculates the coordinates of the atoms of the cluster and defines the shells of atoms. The program creates the muffin-tin potential, finding the muffin-tin radii R_{MT} and the intersphere potential V_{0i} by using the criterion of touching muffin-tin spheres and minimum discontinuity of the muffin-tin potentials for the determination of the intersphere energy. The program always finds a single solution with crystals formed by one (such as rare-gas solids) or two atomic species. In the case of more complex crystals with more than two atomic species and complex structure, two or more minima can be found, and at this point the program asks for a choice.

The input information for the G4XANES program for the calculation of the Ne K -edge XANES are the fcc crystal symmetry of solid Ne with a lattice parameter equal to 4.426 Å,³² and the size of the cluster of neighbor atoms. The structure of a six-shell cluster is reported in Table I. The automatic procedure for the muffin-tin potential construction was described elsewhere.^{33,34} The values of muffin-tin sphere radii R_{MT} and muffin-tin energy constants V_{0i} for both ground-state (unrelaxed) and fully relaxed (see below) cases are reported in Table II.

The other input information we must give to the program is the highest orbital momentum l to be included in the phase shift calculation. In the present calculation, we have included the phase shifts with orbital momenta up to 4, but even for $l_{max} = 3$ there are almost no changes in spectra. The only difference between the spectra with $l_{max} = 4$ and $l_{max} = 3$ is a very small variation in the relative intensity of peaks in the energy region $E > 50$ eV, but these changes become negligible when one takes into account all factors that cause the broadening of the spectra (i.e., the final lifetime of the core hole, the mean free path of the photoelectron, and the experimental resolution).

We have used the procedure of including the broadening terms as the last step before comparison with the experimental spectrum. We have used a constant imaginary part of the potential equal to -0.002 Ry. In all figures, we have reported the normalized absorption

TABLE I. Structure of the cluster used in the calculation.

Number of shells	Number of atoms	Shell radius R (Å)
0	1	
1	13	3.131 78
2	19	4.428 99
3	43	5.424 39
4	55	6.263 55
5	79	7.002 87
6	87	7.671 25

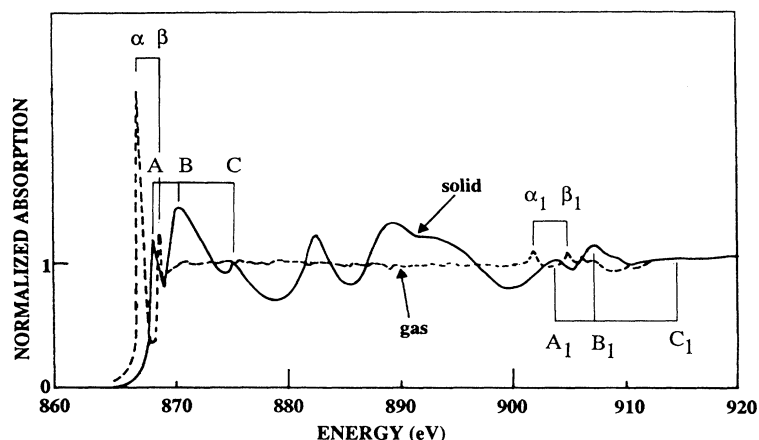


FIG. 1. Ne x-ray-absorption spectra above the K edge in solid-state (Ref. 29) (solid line) and gas (Ref. 8) (dashes) phases.

coefficient (i.e., the absorption coefficient in the relative units of atomic absorption α_0 at high energy). Therefore it is possible to obtain the absolute value of the absorption coefficient by multiplying these normalized data by the value of the atomic absorption jump.

III. RESULTS AND DISCUSSION

In Fig. 1, the neon K -edge XANES spectra of both solid²⁹ and gas⁸ phases are shown. The main difference between the two spectra above the continuum threshold is due to the solid-state term, i.e., to the multiple scattering of the excited photoelectron by neighbor atoms of the absorbing atom in the Ne crystal. The only visible structure existing in the continuum region of the Ne gas are sharp low-intensity maxima, indicated in Fig. 1 as α_1 and β_1 , that Esteva *et al.*⁸ have identified as two-electron excitations corresponding to the transition from $1s^2 2s^2 2p^6$ to $1s^1 2s^2 2p^5 3p^2$ final states. In the spectrum of the solid-state phase at nearly the same energy separation from the main absorption edge, there are also maxima (labeled A_1 , B_1 , and C_1) that can be identified with two-electron excitations, but in order to separate them from the one-electron excitation multiple-scattering resonances, it is necessary to obtain the latter from exact theoretical calculation of the one-electron cross section.

First, we have studied the effects of the size of the cluster on the XANES spectrum. In Fig. 2(a), we show the XANES spectra calculated by considering clusters containing up to five shells. The XANES multiple-scattering analysis has shown^{35,36} that in the case of high-symmetry structures, such as fcc, one must take into account a very large cluster containing up to 10 atoms. In these systems, even when the number of the shells is increased from four

to five, new features appear. The need for large clusters in the interpretation of K -edge XANES of ZnS and NaCl has been reported recently.^{37,38}

We must remark that our results, shown in Fig. 2(a), correspond to the ground state of the solid Ne electronic system. In the energy interval we used, the dipole transition-matrix element is nearly constant versus energy [see Fig. 2(b)], therefore, the curves in Fig. 2(a) are modulated by the p -electron density of states in the con-

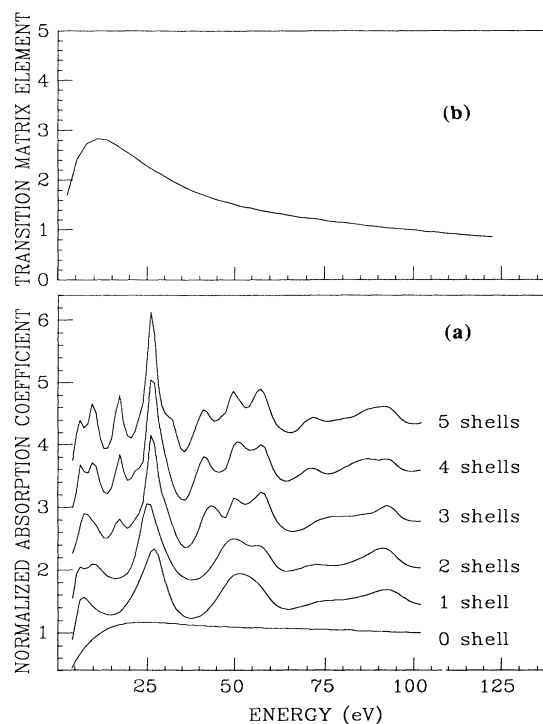


FIG. 2. (a) Normalized x-ray-absorption coefficient for solid Ne near the K edge within a cluster of different size. The origin of the energy scale corresponds to the muffin-tin zero. Each spectrum is shifted along the y axis by the value of 0.5 in relation to the previous one. (b) The dipole transition-matrix element in arbitrary units for K -edge XANES in solid Ne.

TABLE II. The muffin-tin radii R_{MT} and muffin-tin constants V_{0i} according to our calculation.

Atom	R_{MT} (\AA)		V_{0i} (eV)	
	Unrelaxed	Relaxed	Unrelaxed	Relaxed
Ne (central)	1.566	1.880	-3.596	-7.503
Ne (other)	1.566	1.090	-3.596	-7.334

duction band of solid Ne.

The energy-band structure of solid neon has been calculated previously by means of the orthogonalized plane-wave (OPW) method,³⁹ the augmented-plane-wave (APW) method,^{40,41} the Korringa-Kohn-Rostoker (KKR) method,⁴² the APW method with Hedin-Lundqvist exchange,⁴³ and the linear APE (LAPW) method with a self-interaction-correlated local-spin-density approximation.⁴⁴ But only in Ref. 43 was the total density of states reported. In the other works, only the dispersive bands or the energy of some high-symmetry points in the Brillouin zone are reported. This seriously limits the use of these theoretical results for understanding the data of a large number of experimental techniques, where the total or partial density of states are involved.

In order to compare our results with experimental data, we must take into account that the excited photoelectron moves in the presence of the core hole. In the case of insulating materials, it leads to the appearance of the so-called core excitons in the lowest-energy region of XANES.^{45,46} We have assumed that the electronic system of solid Ne is fully relaxed in the field of the $1s$ core hole, and we have treated this situation in the frame of $Z+1$ approximation,¹ i.e., while constructing the muffin-tin potential we have used (for the central atom in the cluster) the atomic electron density of the Na atom. In Fig. 3, we compare the results for the fully relaxed case and those for the unrelaxed one (i.e., corresponding to the initial state of the electronic system). The main differences appear in the lowest-energy part of the XANES spectrum.⁴⁷

We have included all factors that result in the broadening of the spectrum to compare the theoretical spectrum with the experimental data from Ref. 29 (see Fig. 4): (1) a constant term of 0.4 eV, due to the core-hole lifetime and the experimental resolution, and (2) the energy-dependent term that corresponds to the mean free path of the photoelectron in the solid phase. We have used the averaged

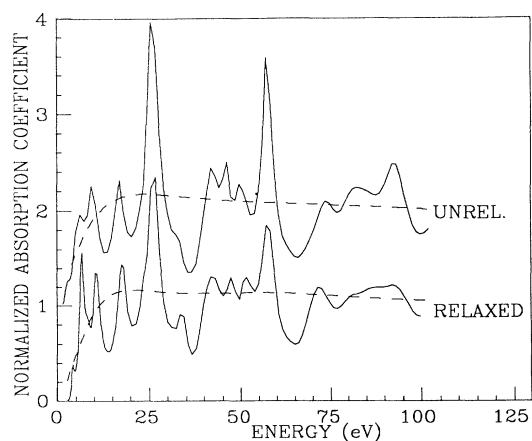


FIG. 3. The normalized x-ray-absorption coefficient for solid Ne calculated at unrelaxed and fully relaxed approximations together with corresponding atomic absorption coefficients. The energy scale zero was chosen at the muffin-tin energy.

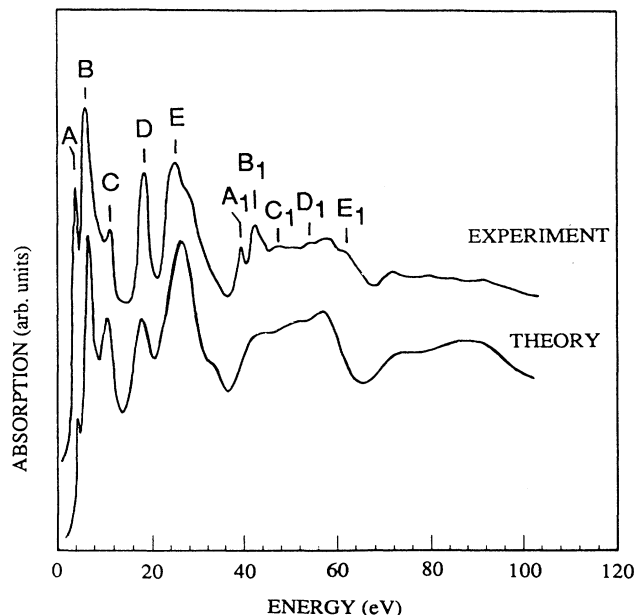


FIG. 4. A comparison of experimental K -XANES in solid Ne (Ref. 29) with the present theoretical results. In contradiction to other figures, theoretical spectra have been calculated taking into account factors that result in the broadening of XANES (see text).

mean free path of the photoelectron function for metals, which is expected to be a poor approximation. In spite of these approximations, one can see that the agreement between the theoretical and experimental results (in the energy region from the main edge up to about 40 eV) is rather good.

Sharp peaks in the experimental spectrum that are not reproduced in the theoretical spectrum appear beyond an energy of about 35 eV. Due to the similarity to the first sharp peaks at the absorption threshold, these absorption peaks have been associated with two-electron excitation in the central atom corresponding to $1s^2 2s^2 2p^6 - 1s^1 2s^2 2p^5 \epsilon_i p^2$ states. One can see in Fig. 4 that each one-electron excitation multiple-scattering maximum (labeled A , B , C , D , and E) corresponding to $1s^2 2s^2 2p^6 \rightarrow 1s^1 2s^2 2p^5 \epsilon_i p^1$ transitions has its own two-electron excitation "replica" (labeled A_1 , B_1 , C_1 , D_1 , and E_1) and corresponding to $1s^2 2s^2 2p^6 \rightarrow 1s^1 2s^2 2p^5 \epsilon_i p^2$ transitions. This interpretation is confirmed by the sharp character of these features in comparison to the bandwidth of the one-electron excitation multiple-scattering resonances at an energy about 30 eV above the main edge, which are broader according to the small value of the photoelectron mean free path for this energy. In the XANES spectra of heavier rare-gas solids [for example, in solid Kr XANES (Ref. 30)], the double excitations are difficult to resolve in the XANES spectrum because of the decreasing relative probability of two- and one-electron excitations with increasing atomic number.⁴⁸ But in the case of the absence of XANES modulation, i.e., in the gas phase, one can see the two-electron peaks

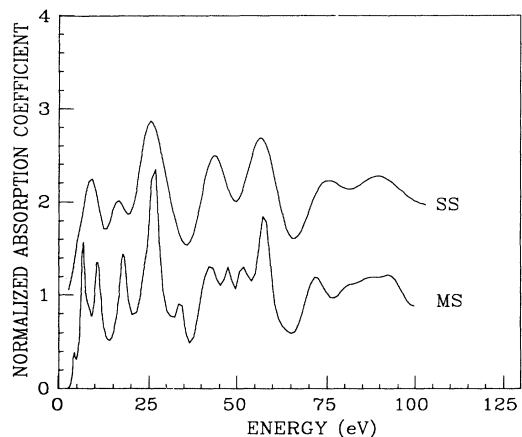


FIG. 5. The normalized x-ray-absorption coefficient for solid Ne calculated within the full multiple-scattering (MS) approach, and taking into account only single-scattering (SS) pathways of the photoelectron.

in the x-ray-absorption spectrum of Kr (Ref. 49) at an energy of about 20 eV above the absorption edge.

In order to study the validity of the single-scattering (SS) approximation (widely used for EXAFS interpretation) for x-ray absorption in solid Ne, we have also performed a single-scattering calculation for the fully relaxed case. As one can see from Fig. 5, the single-scattering approximation gives broad features that are in some correspondence with the full multiple-scattering results, but it is unable to describe the lowest-energy region of the spectrum.

Previously, valence excitons in solid Ne,^{27,40,45} Kr,⁵⁰ Ne, Ar, Kr, and Xe,⁴⁶ and shallow core-level excitons^{39,51,52} were investigated. In Fig. 1, one can observe the energy shift of the first two peaks from the gas phase

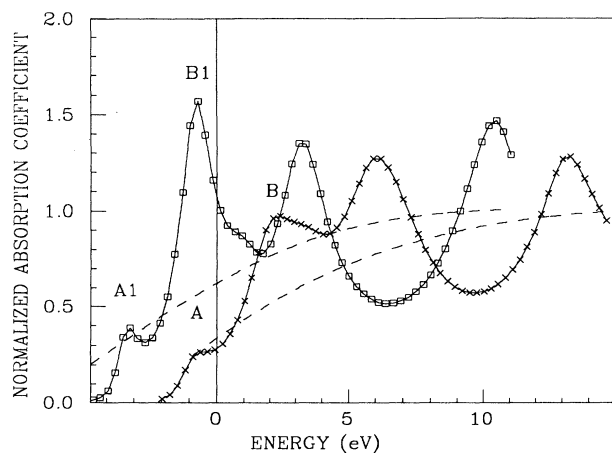


FIG. 6. The normalized x-ray-absorption coefficient for solid Ne calculated at the unrelaxed (crosses) and fully relaxed (squares) potentials together with the corresponding atomic absorption coefficients. The zero of the energy scale was chosen at the vacuum-level energy.

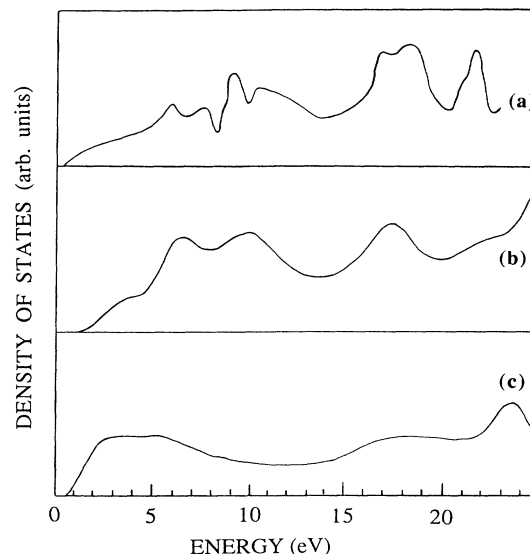


FIG. 7. (a) The total density of states of solid Ne from Ref. 43. (b) The p -projected and (c) s -projected density of states in solid neon obtained in the present work.

to the solid phase, which is due to the reduction of the binding energy of the bound states in the solid because of the dielectric response of the condensed system (namely the core-hole screening by the valence electrons). This energy shift is 1.2 eV for the lowest peak and 0.8 eV for the next one.⁹

In Fig. 6, we report the theoretical transition rate obtained for both unrelaxed (corresponding to the ground state) and fully relaxed (corresponding to the x-ray-absorption final state) potentials. In the transition rate curve of the unrelaxed ground-state potential, there exist two features (labeled A and B) corresponding to the first ones in the fully relaxed potential (labeled A_1 and B_1). The first sharp maxima in solid rare gases are generally treated as "core excitons." The existence of the corresponding features in the ground state shows that for the description of the first two maxima in solid Ne absorption spectra, one can use the concept of "bound states" instead of "core excitons." It is well known that the bottom of the conduction band in the ground state of solid Ne is formed with s states. In order to control the relative position of the p electronic states, we have calculated the transitions to s states (i.e., $2p \rightarrow \epsilon s$). These results are compared in Fig. 7 with the total density of states obtained recently.⁴³

IV. CONCLUSIONS

In conclusion, we have identified, in solid Ne K -edge XANES data, the spectral features corresponding to one-electron excitations of the photoelectron to the final states as well as the two-electron excitations. The intensity of the two-electron excitations in the solid state, as shown in Fig. 4, are so strong that they have to be

identified and eliminated before analysis of the EXAFS data, eventually extended to low energy, by taking the Fourier transform in order to avoid spurious results. We must remark that the energy range of two-electron excitations can be predicted easily by atomic theory; therefore, before an EXAFS data analysis of a core level, one

should first search for the two-electron excitations in the expected energy range.

We have also succeeded in predicting the lowest-energy peak at the *K* edge, known as the "core exciton," which is shown to be due to the lowest unoccupied valence state pushed down in the bound-state region by the core hole.

- *Permanent address: Department of Solid State Physics, Rostov University, Sorge strasse 5, 344104 Rostov-Don, Russia.
- ¹A. Bianconi, in *X-Ray Absorption: Principle, Applications, Techniques of EXAFS, SEXAFS, XANES*, edited by R. Printz and D. Koningsberger (Wiley, New York, 1988), p. 573.
- ²A. Bianconi, J. Garcia, and M. Benfatto (unpublished).
- ³H. W. Schnopper, *Phys. Rev.* **131**, 2558 (1963).
- ⁴C. Bonnelle and F. Wuilleumier, *C. R. Acad. Ser. B* **256**, 5106 (1963).
- ⁵R. D. Deslattes, R. E. Lavilla, P. L. Cowan, and A. Henis, *Phys. Rev. A* **27**, 923 (1983).
- ⁶G. Bradley Armen, T. Aberg, K. R. Karim, J. C. Levin, B. Crasemann, G. S. Brown, M. H. Chen, and G. E. Ice, *Phys. Rev. Lett.* **54**, 182 (1985).
- ⁷F. Wuilleumier and C. Bonnelle, *C. R. Acad. Ser. B* **270**, 1229 (1970).
- ⁸J. M. Esteve, B. Gauthe, P. Dhez, and K. R. Karnatak, *J. Phys. B* **16**, L263 (1983).
- ⁹F. Wuilleumier, *C. R. Acad. Ser. B* **263**, 449 (1966); Y. Ito, H. Nakamatsu, T. Mukoyama, K. Omote, S. Yoshikato, M. Takahashi, and S. Emura (unpublished).
- ¹⁰Xe Zhang, E. A. Stern, and J. J. Rehr, in *XAFS and Near Edge Structure III*, edited by K. O. Hodgson, B. Hedman, and J. E. Penner Hahn (Springer-Verlag, Berlin, 1984), p. 18.
- ¹¹M. H. Tuiller, D. Laporte, and J. M. Esteve, *Phys. Rev. A* **26**, 373 (1982).
- ¹²S. Bodeur, P. Millie, E. Lizon à Lugrin, I. Nenner, A. Filipponi, F. Boscherini, and S. Mobilio, *Phys. Rev. A* **39**, 5075 (1989).
- ¹³U. Fano and J. W. Cooper, *Rev. Mod. Phys.* **40**, 441 (1968).
- ¹⁴J. J. Rehr, E. A. Stern, R. L. Martin, and E. R. Davidson, *Phys. Rev. B* **17**, 560 (1978).
- ¹⁵A. Filipponi, E. Bernieri, and S. Mobilio, *Phys. Rev. B* **38**, 3298 (1988).
- ¹⁶M. Deutsch and M. Hart, *Phys. Rev. A* **29**, 2946 (1984).
- ¹⁷S. I. Salem, Brahm Dev, and P. L. Lee, *Phys. Rev. A* **22**, 2679 (1980).
- ¹⁸S. I. Salem, A. Kumar, K. G. Schiessel, and P. L. Lee, *Phys. Rev. A* **26**, 3334 (1982).
- ¹⁹S. I. Salem, A. Kumar, and P. L. Lee, *Phys. Rev. A* **25**, 2069 (1982).
- ²⁰S. I. Salem and A. Kumar, *J. Phys. B* **19**, 73 (1986).
- ²¹G. Li, F. Bridges, and G. S. Brown, *Phys. Rev. Lett.* **68**, 1609 (1992).
- ²²A. Bianconi, J. Garcia, M. Benfatto, A. Marcelli, C. R. Natoli, and M. F. Ruiz-Lopez, *Phys. Rev. B* **43**, 6885 (1991).
- ²³M. J. Puska and R. M. Nieninen, *J. Phys. Condens. Matter* **3**, 5711 (1991).
- ²⁴R. V. Vedrinskii and I. I. Gegusin, *X-Ray Absorption Spectroscopy of Solids* (Energoatomizdat, Moscow, 1991).
- ²⁵R. Haensel, G. Keitel, P. Schreiber, and C. Kunz, *Phys. Rev.* **188**, 1375 (1969).
- ²⁶R. Haensel, G. Keitel, E. E. Koch, M. Skibowski, and P. Schreiber, *Phys. Rev. Lett.* **23**, 1160 (1969).
- ²⁷R. Haensel, G. Keitel, C. Kunz, and P. Schreiber, *Phys. Rev. Lett.* **25**, 208 (1970).
- ²⁸V. A. Yavna, A. N. Hopersky, A. M. Napolinsky, and V. A. Popov, *Proceedings of the Second European Conference on Progress in x-Ray Synchrotron Radiation Research* (SIF, Bologna, 1990), p. 101.
- ²⁹A. Hiraya, K. Fukui, P.-K. Tseng, T. Murata, and M. Watanabe, *J. Phys. Soc. Jpn.* **60**, 1824 (1991).
- ³⁰A. Polian, J. P. Itie, E. Dartyge, A. Fontaine, and G. Tourillon, *Phys. Rev. B* **39**, 3369 (1989).
- ³¹P. Durham, in *X-Ray Absorption: Principle, Applications, Techniques of EXAFS, SEXAFS, XANES* (Ref. 1), p. 53.
- ³²R. W. G. Wyckhoff, *Crystal Structures* (Interscience, New York, 1965).
- ³³C. Li, M. Pompa, A. Congiu-Castellano, S. Della Longa, and A. Bianconi, *Physica C* **175**, 369 (1991); M. Pompa, C. Li, A. Bianconi, A. Congui-Castellano, S. Della Longa, A.-M. Flank, P. Lagarde, and D. Udron, *ibid.* **184**, 51 (1991); C. Li, M. Pompa, S. Della Longa, and A. Bianconi, *ibid.* **178**, 421 (1991).
- ³⁴A. Bianconi, C. Li, F. Campanella, S. Della Longa, I. Pettiti, M. Pompa, S. Turtu, and D. Udron, *Phys. Rev. B* **44**, 4560 (1991); A. Bianconi, C. Li, M. Pompa, A. Congiu-Castellano, S. Della Longa, D. Udron, A.-M. Flank, and P. Lagarde, *ibid.* **44**, 10 126 (1991); A. Bianconi, C. Li, S. Della Longa, and M. Pompa, *ibid.* **45**, 4989 (1992).
- ³⁵A. Bianconi, A. V. Soldatov, and T. S. Ivanchenko, *Nucl. Instrum. Methods A* **308**, 248 (1991); A. V. Soldatov, Yu. V. Sukhetsky, and A. Bianconi, *ibid.* **308**, 246 (1991).
- ³⁶A. V. Soldatov, T. S. Ivanchenko, S. Della Longa, and A. Bianconi, *Phys. Status Solidi B* **168**, k43 (1991).
- ³⁷Ph. Sainctavit, J. Petiau, M. Benfatto, and C. Natoli, *Physica B* **158**, 347 (1989).
- ³⁸R. Gunnella, M. Benfatto, A. Marcelli, and C. R. Natoli, *Solid State Commun.* **76**, 109 (1990).
- ³⁹S. Baroni, G. Grosso, and G. P. Parravicini, *Phys. Rev. B* **22**, 6440 (1980).
- ⁴⁰W. Andreoni, F. Perrot, and F. Bassani, *Phys. Rev. B* **14**, 3589 (1976).
- ⁴¹U. Rossler, *Phys. Status Solidi* **42**, 345 (1970).
- ⁴²S. Natalizi and R. Resta, *J. Phys. C* **10**, 1477 (1977).
- ⁴³N. C. Bacalis, D. A. Papaconstantopoulos, and W. E. Pickett, *Phys. Rev. B* **38**, 6218 (1988).
- ⁴⁴Y. Li, J. B. Krieger, M. R. Norman, and G. J. Iafrate, *Phys. Rev. B* **44**, 10 437 (1991).
- ⁴⁵E. Boursey, J.-Y. Roncin, and H. Damaney, *Phys. Rev. Lett.* **25**, 1279 (1970).
- ⁴⁶D. Pudewill, F. J. Himpsel, V. Saile, N. Schwentner, M. Skibowski, and E. E. Koch, *Phys. Status Solidi B* **74**, 485 (1976).
- ⁴⁷O. Keski-Rahkonen and M. O. Krause, *At. Data Nucl. Data Tables* **14**, 139 (1974).
- ⁴⁸M. O. Krause, *J. Phys. (Paris) Colloq.* **32**, C4-67 (1971).

- ⁴⁹T. Hayaishi, E. Murakami, Y. Morioka, E. Shigemasa, A. Yagishita, H. Aksela, and S. Aksela, Photon Factor Rep. **8**, 244 (1990).
- ⁵⁰V. Saile, R. Reininger, R. Laporte, I. T. Steinberger, and G. L. Findley, Phys. Rev. B **37**, 10 901 (1988).
- ⁵¹L. Resca, R. Resta, and S. Rodriguez, Phys. Rev. B **18**, 702 (1978).
- ⁵²L. Resca, Phys. Rev. B **37**, 10 898 (1988).